Calciothermic Reduction of Titanium Oxide and *in-situ* Electrolysis in Molten $CaCl_2$

RYOSUKE O. SUZUKI, KOH TERANUMA, and KATSUTOSHI ONO

A concept for calciothermic direct reduction of titanium dioxide in molten $CaCl_2$ is proposed and experimentally tested. This production process consists of a single cell, where both the thermochemical reaction of the calciothermic reduction and the electrochemical reaction for recovery of the reducing agent, Ca, coexist in the same molten $CaCl_2$ bath. A few molar percentages of Ca dissolve in the melt, which gives the media a strong reducing power. Using a carbon anode and a Ti basket-type cathode in which anatase-type TiO_2 powder was filled, a metallic titanium sponge containing 2000 ppm oxygen was produced after 10.8 ks at 1173 K in the $CaCl_2$ bath. The optimum concentration of CaO in the molten $CaCl_2$ was 0.5 to 1 mol pct, to shorten the operating time and to achieve a lower oxygen content in Ti.

I. INTRODUCTION

THE Kroll process produces metallic titanium industrially. It consists of a three-step operation: the conversion from TiO_2 to $TiCl_4$, the subsequent reduction of $TiCl_4$ to sponge Ti by liquid Mg, and the electrochemical recycling of $MgCl_2$ into metallic Mg.[1] It takes 2 to 5 days in this reduction route *via* $TiCl_4$, and the batch operation makes it difficult to save thermal energy. A simpler, more rapid, and compact process in a single step directly from TiO_2 has been desired to achieve higher productivity and energy savings.[2–8]

Recently, we proposed briefly the possible routes to go from TiO_2 directly to metallic Ti, using calcium as a reductant and $CaCl_2$ as the supporting media.[4–8] The purpose of this article is to report our concept in detail and to show some experimental verification.

II. CONCEPT

A. *Thermodynamic Requirements*

The possible elements that are candidates as reductants (R) of TiO_2 should meet several requirements. First, the oxides of the reductants (RO) should be thermodynamically more stable than the lowest oxide of titanium, TiO.

$$\mathrm{TiO} + R = \mathrm{Ti} + RO \qquad [1]$$

where R is selected judging from the standard free-energy change of Reaction [1] (ΔG°[1]) from a thermodynamic database.[9]

Second, a reductant with a wide solubility in Ti or with a strong compound formability with Ti is not suitable. For example, α-Ti dissolves 44.8 mol pct Al, and the residual amount of reductant Al forms a Ti-Al alloy. Carbon is one of the common reductants, but is not applicable because of TiC formation. Table I lists elements which can reduce TiO, whose solubility in Ti does not exceed 5 mol pct[10] and which do not make any compounds with Ti.

RYOSUKE O. SUZUKI, Associate Professor, and KATSUTOSHI ONO, Professor Emeritus, are with the Department of Energy Science and Technology, Kyoto University, Kyoto, Japan. Contact e-mail: Suzuki@energy.kyoto-u.ac.jp KOH TERANUMA, formerly Graduate Student, Master Course of Graduate School of Energy Science, Kyoto University, is Research Staff Member with Toho Gas Company, Nagoya, Japan.

Manuscript submitted August 23, 2002.

The third criterion is the deoxidation capacity. For example, Mg equilibrates thermodynamically with Ti containing about 2 to 3 mass pct oxygen,[11,12] and a subsequent deoxidation procedure is needed after reduction with Mg. In addition, the acid leaching of MgO was too slow for practical mass production.[13] Rare-earth elements are not suitable as reductants if they cannot be recycled inside the operating system. Radioactive or noxious elements are excluded as TiO_2 reductants.

Ca was selected as being applicable both for direct reduction of TiO_2 and for deoxidation of Ti. The residual oxygen in Ti has been measured as 300 to 730 mass ppm, when Ca and CaO coexisted in equilibrium at 1173 to 1373 K.[11,12,14–18] This oxygen level is suitable for industrial purposes. The solubility of Ca in β-Ti is also as low as 50 to 200 ppm at 1155 to 1600 K.[19]

Alexander first patented the reduction of TiO_2 using Ca in 1936.[20] However, ductile titanium could not be produced,[13] because a few thousand parts per million oxygen remained in the formed Ti.[12,14–16] The slow mass transfer through the byproduct CaO, attached to the surface of Ti particles, hindered further deoxidation.[12,14–16] The formed Ti particles easily sintered tightly, because reaction [1] is exothermic.[9] CaO was easily captured in the Ti grain boundaries during sintering and was barely removed by acid leaching.[12,14–16]

B. *Calciothermic Reduction in Molten $CaCl_2$*

Calcium chloride ($CaCl_2$) is an abundant and inexpensive salt which melts at 1048 K and is thermodynamically stable with Ca. CaO solubility in molten $CaCl_2$ is about 20 mol pct CaO at 1173 K.[21–24] When we applied the calciothermic reduction in the molten $CaCl_2$, the byproduct CaO was removed *in situ* from the reaction place and dissolved into the salt, which enhanced the reduction,[2–8] as illustrated in Figure 1.

$$\mathrm{TiO_2} + 2\ \mathrm{Ca} = \mathrm{Ti} + 2\ \underline{\mathrm{CaO}} \qquad [2]$$

where $\underline{\mathrm{CaO}}$ represents the dissolved CaO in the salt. Note that the solidified $CaCl_2$ is more easily separated from Ti powder with water than is CaO with acid leaching. $CaCl_2$ could supply Ca toward the oxides homogeneously,[25] and the molten salt released the exothermic heat from the reaction.[25,26] The simultaneous usage of Ca and $CaCl_2$ in oxide

Table I. Possible Reductants to Produce Ti Metal from its Oxide, Considering the Thermodynamic Reaction, Equation [1], and Formation of Alloy or Compounds

Group	Possible Reductants
Ia	Li
IIa	Be, Mg, Ca, Sr, Ba
IIIa	Sc, Y, La, Ce, Pr, Nd, (Pm),* Sm, Eu, Gd, Tb, Dy, Ho, Er, Tm, Yb, Lu, Ac, Th

*No thermochemical data are available.

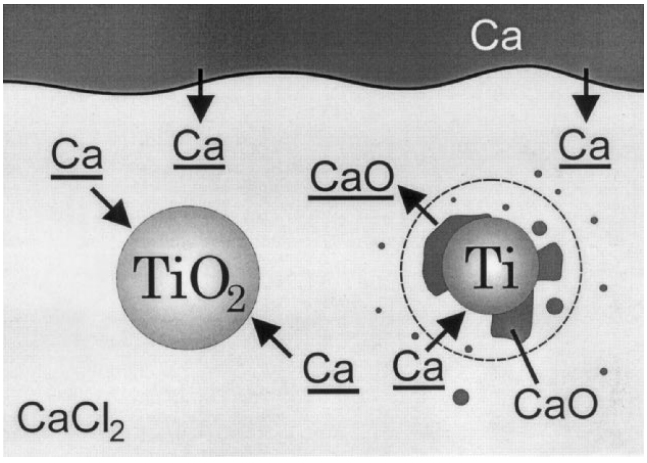

Fig. 1—Mechanism of calciothermic reduction.

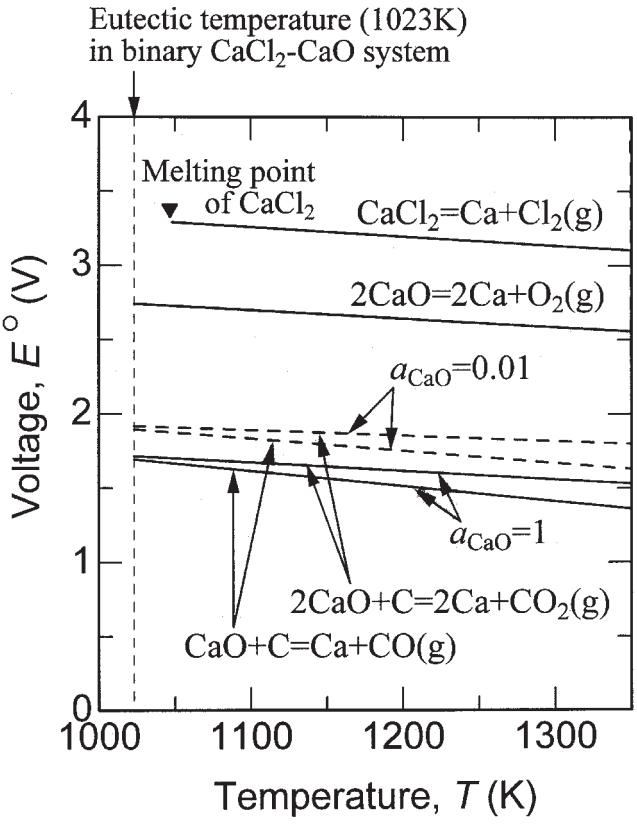

Fig. 2—Electrochemical potentials for the decomposition of $CaCl_2$ and that of CaO in $CaCl_2$.

reduction was reported only at the production of Pu,[26] Nd, an Fe-Nd alloy,[27,28,29] or Nb-Ti alloys.[25]

The densities of liquid Ca and $CaCl_2$ at 1173 K are 1.357×10^3 and 2.01×10^3 kg/m^3, respectively,[30] which separates into two layers. As illustrated in Figure 1, TiO_2 does not come into contact with Ca, because the densities of rutile-type TiO_2 and β-Ti at 1173 K are evaluated as 4.40×10^3 and 4.15×10^3 kg/m^3, respectively.[30,31] Ca dissolved in molten $CaCl_2$ (the solubility of Ca is 2 to 4 mol pct[32–38]) could reduce TiO_2 powder experimentally.[4–8]

$$TiO_2 + 2\,\underline{Ca} = Ti + 2\,\underline{CaO} \qquad [3]$$

where Ca represents dissolved calcium. Pure Ca is not necessary to reduce TiO_2 into the metallic Ti, and Ca formed electrochemically can be used for TiO_2 reduction, as shown in this work.

C. *Electrolysis of CaO in Molten $CaCl_2$*

In order both to enhance CaO dissolution and to recycle the byproduct CaO, the dissolved CaO is removed from the salt and decomposed to metallic Ca, using the electrochemical reaction in the molten salt.[3,8,39–41] CaO is decomposed into ions as

$$\underline{CaO} = \underline{Ca^{2+}} + \underline{O^{2-}} \qquad [4]$$

The electrochemical potential necessary for CaO decomposition is evaluated in Figure 2 from a thermochemical database.[9] Because the theoretical decomposition voltage of CaO into O_2 gas and Ca (2.71 V at 1173 K) is lower than that of $CaCl_2$ (3.213 V), Ca can be produced by the molten-salt electrolysis of CaO. This oxygen-gas evolution, however, requires an oxidation-resistive material such as a nonconsumable anode material. The decomposition voltage of CaO is close to that of $CaCl_2$, and the overpotential makes it difficult to exclude Cl_2 gas evolution. Instead of using a nonconsumable anode for O_2 gas evolution, a consumable carbon anode can lower the potential by 1.03 V.[4–6,8,39–41]

$$\text{At the anode: } C + 2\,\underline{O^{2-}} = CO_2\,(gas) + 4e^-,\ C + \underline{O^{2-}} = CO\,(gas) + 2e^- \qquad [5]$$

$$\text{At the cathode: } \underline{Ca^{2+}} + 2e^- = Ca \qquad [6]$$

Even in case of a low activity of CaO (a_{CaO}), the decomposition voltage of CaO remains much lower than that of $CaCl_2$ decomposition, as shown in Figure 2.

Many previous attempts of $CaCl_2$ or CaO electrolysis were reported.[22,24,28,39–44] However, it was not easy to deposit either pure liquid Ca or a liquid Ca alloy with a good yield and a good current efficiency, because the precipitated Ca dissolved immediately back into the salt and parasitic reactions occurred. During electrolysis at temperatures above the melting point of Ca, the formation of a so-called "metal fog" of Ca has been often observed in the vicinity of the cathode.[22,43,44] This metal fog holds the reducing potential to cause the parasitic reactions. Some earlier reports suggested "Ca_2^{2+},"[34,45] while the later studies showed Ca^+ or $(Ca^{2+} + e)$.[33,46]

$$\text{At the cathode: } Ca^{2+} + e^- = Ca^+ \qquad [7]$$

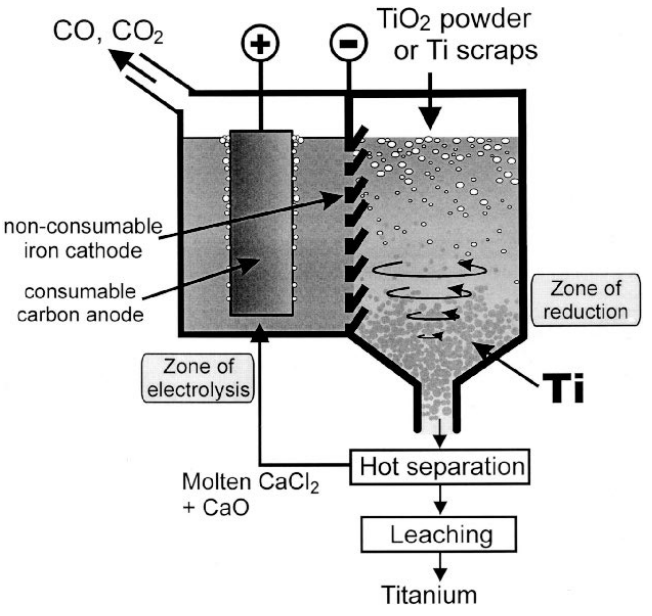

Fig. 3—Illustration of single cell model.

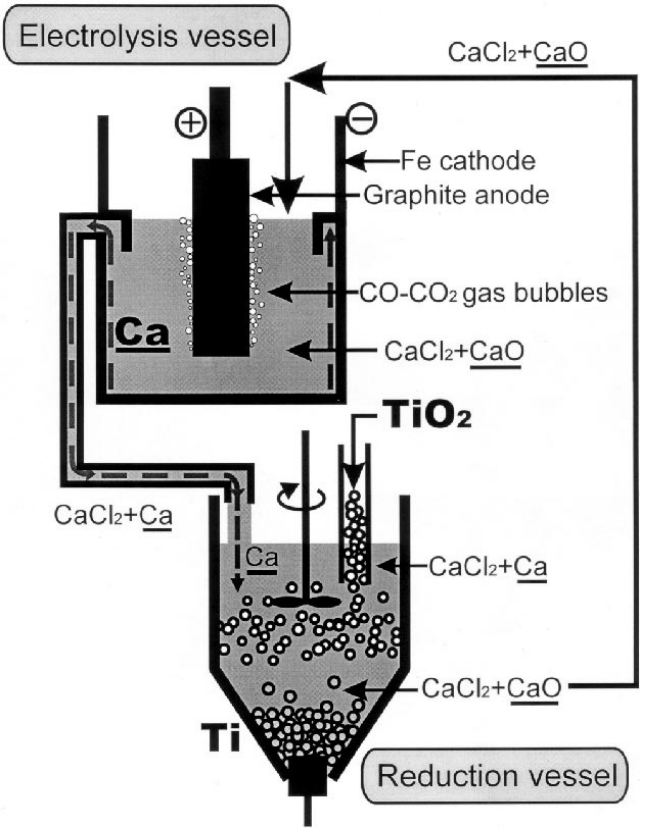

Fig. 4—Illustration of separate model.

The Ca^{+} ions leave the cathode and migrate to the bulk. Because of their reducing power, they are finally neutralized by parasitic reactions such as

$$\text{In the bath: } 2Ca^{+} + CO_2\,(\text{gas}) + 2e^{-} = 2Ca^{2+} + 2O^{2-} + C \text{ and,} \quad [8]$$

$$\text{In the bath: } Ca^{+} + CO\,(\text{gas}) + e^{-} = Ca^{2+} + O^{2-} + C \quad [9]$$

In this article, we will call Ca_2^{2+} or Ca^{+} ions as Ca dissolved in the salt "Ca," to express the reducing ability or potential near the cathode, no matter which is the so-called metal fog after deposition—the ionic state such as Ca_2^{2+} or, simply, dissolved metallic calcium. This reducing atmosphere of Ca is thermochemically equivalent to Ca in Eq. [2] and served here for the reduction of TiO_2 instead of the parasitic Reactions [8] and [9]. We will put TiO_2 powder at the vicinity of the cathode (Figure 3) to consume Ca in the molten salt, as written in Eq. [3].

D. *Combination of Reduction and Electrolysis*

The electrolysis and reduction can be combined together, as illustrated in Figure 4. The conceptual image of the two reaction vessels (Figure 4) was proposed in calciothermic reduction of TiO_2, Nd_2O_3, and radioactive elements.[2,3,39–42] Ca or Ca formed at the cathode is passed with a part of the molten salt toward the reduction vessel and is used for the reduction of the oxide powder. The byproduct, CaO, and the solvent $CaCl_2$ are returned to the upper vessel. However, no experimental proof has been reported, probably because of the difficulties of depositing pure Ca by electrolysis. TiO_2 powder could be successfully reduced by Ca as well as by pure Ca.[7] It was not directly proven whether Ca produced by electrolysis could be used for the reduction.

The single-unit operation (Figure 3) is ideal; it omits the connection paths between two vessels, and the Ca is served instantly for TiO_2 reduction. The reduction is operated in the temperature range of 1120 to 1350 K, considering the melting point and evaporation of Ca. The electrolysis is also conducted in the similar temperature range. Because the calciothermic reduction and the electrolysis are exothermic and endothermic, respectively, thermal energy can be saved by setting two reactions in a close spatial arrangement such as in Figure 3.[4,5,6]

E. *Deoxidation by Ca*

Metallic Ca can effectively extract the residual oxygen in Ti into $CaCl_2$.[47–51]

$$[O]_{Ti} + Ca = Ca^{2+} + O^{2-} \quad [10]$$

where $[O]_{Ti}$ is oxygen in the Ti particles (maximum of 14 mass pct). When we could reduce TiO_2 to Ti powder in Eq. [3], the obtained Ti powder would be simultaneously deoxidized by Eq. [10]. This deoxidation proceeds effectively when the CaO concentration is low. Our previous report showed that the oxygen content in Ti powder just reduced from TiO_2 decreased to <1000 ppm in 1 hour and to 420 ppm in 1 day.[7,8] However, the amount of CaO in the melt after the reduction would be much larger than that suitable for deoxidation. When the CaO concentration becomes higher than 5 mol pct, the dissolution rate of Ca and CaO becomes slower.[24,34,38]

The electrolysis of CaO can decrease the CaO concentration in the melt, and the oxygen content in Ti cathode wires of $[O]_{Ti} > 1000$ ppm O was reported to be decreased to a <30 ppm O level.[52,53] Although the oxygen diffusion became the rate-determining step in the case of the thick wires, we can expect the more-efficient deoxidation in the case of

the fine Ti powder just precipitated from TiO_2. In the single-cell operation (Figure 3), the reduced Ti particles can be also deoxidized by the electrochemical mechanism.[52,53]

F. *Overall Reaction*

Our proposed process starting from TiO_2 is summarized from all the working reactions ([2] through [6] and [10]) that TiO_2 is reduced by carbon as

$$TiO_2 + C = Ti + CO_2 \text{ and } TiO_2 + 2C = Ti + 2CO \quad [11]$$

This overall reaction is the same as that in the Kroll process, where the reductant Mg and the byproducts, $TiCl_4$ and $MgCl_2$, are circulated in a close system.[1]

III. EXPERIMENTAL PROCEDURES

Figure 5 shows the experimental arrangement for the simultaneous reactions, *i.e.,* reduction and *in-situ* electrolysis. A graphite crucible (99.9 pct in metallic purity, 55 mm o.d., 40 mm i.d., and 150 mm in depth) was used as the anode. It was connected to a stainless steel rod (4 mm in diameter) and a lead to a direct-current power supply. About 300 g of a mixture of anhydrate $CaCl_2$ (>99 pct) and CaO (99 pct, calcined at 1473 K in air) was filled in the crucible and heated in vacuum at 623 to 773 K overnight. It was then melted in a purified Ar gas atmosphere and held for 3.6 ks with frequent stirring. The preelectrolysis with a stainless steel or Ti cathode rod at 1.0 to 1.3 V was conducted at 1173 K to eliminate metallic impurities and water.

A pure Ti net (No. 100 mesh) or a SUS304 stainless steel net (No. 250 mesh) was used for the cathode material. It was doubly wound like cylinder (6 to 8 mm i.d. and about 150 mm in length) and tightened by thin Ti wires. The bottom was sealed by a Ti block. About 0.5 to 3 g granular TiO_2 (>99 pct, anatase, primary particle size <1 μm) was filled in this basket-type cathode. The size of the aggregates was about 200 to 800 μm, so that 91.9 pct of them were larger than the No. 100 mesh. The basket-type cathode was connected to a stainless steel pipe (6 or 8 mm o.d.) and a lead to the power supply.

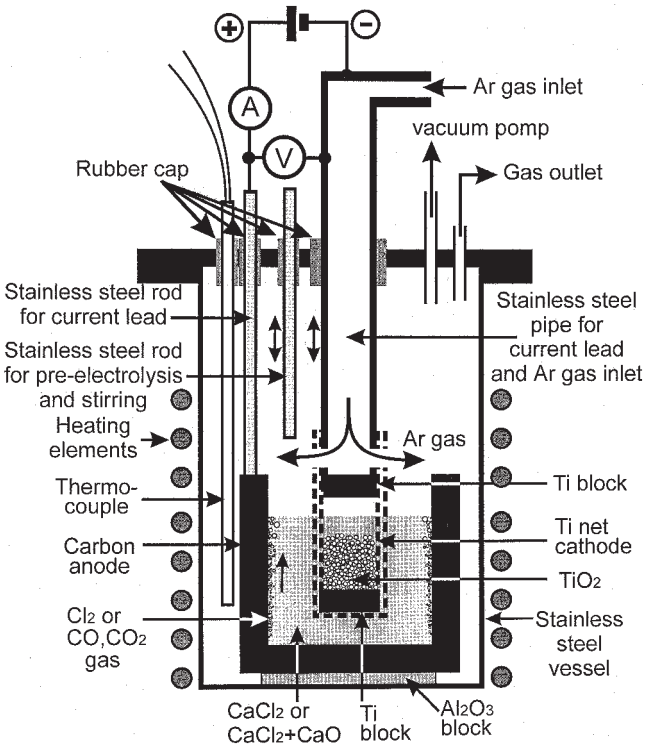

Fig. 5—Experimental setup for TiO_2 reduction.

After pre-electrolysis, the basket-type cathode was immersed in the salt (about 30 to 50 mm in depth) and held at 30 mm above the bottom at 1173 ± 5 K in Ar gas. A direct current was supplied under a constant voltage. The applied voltage between the two electrodes was measured just outside the vessel. Ar gas was blown to the melt surface through the pipe for the cathodic lead. The evolving gas was trapped in an aqueous solution containing $Ca(OH)_2$ or $AgNO_3$ to detect CO_2 or Cl_2 gas, respectively.

After electrolysis, the cathode was taken out of the melt and cooled in Ar gas at the upper part of the furnace. The solidified salt in the basket-type cathode was leached in the flow of drinking water, with cooling below 283 K.[7] The black Ti powder was subsequently rinsed with dilute HCl (or acetic acid), distilled water, and alcohol, in that order, and then dried in vacuum for analysis. The obtained powder was identified by X-ray diffraction (XRD) measurement. The oxygen concentration was analyzed by an inert gas fusion–infrared absorption method. The morphology was observed using scanning electron microscopy (SEM) equipped with an energy-dispersive X-ray (EDX) analyzer.

IV. RESULTS AND DISCUSSIONS

A. *Electrolysis and Reduction above 3.3 V*

During electrolysis above 3.3 V at 1173 K (the decomposition voltage of $CaCl_2$ is 3.213 V[9]), a faint amount of CO_2 gas evolution was detected in addition to a large amount of Cl_2 gas, as listed in Table II. The O_2 and CO gases were not analyzed.

Figure 6 shows the current change during electrolysis. In the early stage (<2 ks), the current dropped rapidly to half of the initial value and then increased gradually. Because of the drop of the bath resistance, the voltage between the electrodes increased slightly during electrolysis, as listed in Table II. The current density was 0.4 to 0.8 × 10^4 A/m^2 for the cathode net area. A small amount of hydrogen gas bubbles were released at all the parts of solidified salt when the salt dissolved in water. It may prove the precipitation of Ca during cooling. The bulk Ca was never found in the basket-type cathode. It is believed that calcium formed by electrolysis dissolved as Ca into the salt.

The sample obtained in the Ti cathode was black and slightly sintered, when it contained α-Ti phase. Figure 7 shows SEM images of the obtained powders, which consisted of α-Ti single phase. The formation of twin structures due to the high oxygen concentration was observed on the particle surface. A lower Ti oxide, $TiO_{0.325}$, was also detected by XRD in the case of short-term electrolysis, although this suboxide is not stable at the operating temperature.[10] We judged that the stable phase at 1173 K (α-Ti) transformed to $TiO_{0.325}$ during cooling, because the oxygen solubility in α-Ti is about 31.9 mol pct.

The analyzed oxygen concentration was relatively high, even when the samples were α-Ti single phase (runs c-1 and c-2). Considering that the reduction by a sufficient amount of Ca could produce α-Ti with 1000 mass ppm O in only 3.6 ks

Table II. Experimental Conditions and Results Using Ti Basket-Type Cathode

Run	Molten Salt (mol pct)	Voltage (V)	Detected Gas	Time (ks)	Total Charge (C)	Phases Identified by XRD	Oxygen Concentration (Mass ppm)	Current Efficiency (pct)
c-1	$CaCl_2$	3.5 to 3.8	Cl_2, (CO_2)	10.8	53 598	α-Ti	6 860	8.8
c-2	$CaCl_2$	3.4 to 3.7	Cl_2, (CO_2)	3.6	17 688	α-Ti	38 000	25.5
c-3	$CaCl_2$	3.5 to 3.7	—	1.8	10 443	α-Ti, $TiO_{0.325}$	—	—
d-1	15 pct CaO	2.6 to 2.8	CO_2	10.8	54 126	α-Ti, $TiO_{0.325}$	—	—
d-2	15 pct CaO	2.3 to 2.9	—	10.8	54 000	α-Ti, TiO?	—	—
d-3	15 pct CaO	2.6 to 2.9	—	10.8	69 396	$TiO_{0.325}$	—	—
d-4	15 pct CaO	2.6 to 2.8	CO_2	3.6	23 055	Ti_6O, TiO	—	—
d-5	15 pct CaO	2.6 to 2.8	CO_2	1.8	10 800	$TiO_{0.325}$, TiO	—	—
e-1	1 pct CaO	2.5 to 2.8	CO_2	10.8	40 194	α-Ti	6 190	11.8
e-2	1 pct CaO	2.6 to 2.8	CO_2	3.6	14 931	α-Ti, $TiO_{0.325}$	—	—
f-1	0.5 pct CaO	2.6 to 2.9	CO_2	10.8	36 978	α-Ti	2 000	12.9
f-2	0.5 pct CaO	2.7 to 2.9	CO_2	3.6	10 704	α-Ti, $TiO_{0.325}$	—	—
g-1	$CaCl_2$	2.6 to 2.8	CO_2	10.8	25 374	$TiO_{0.325}$	—	—
g-2	$CaCl_2$	2.6 to 2.9	CO_2	3.6	5 439	$TiO_{0.325}$	—	—

—not measured.

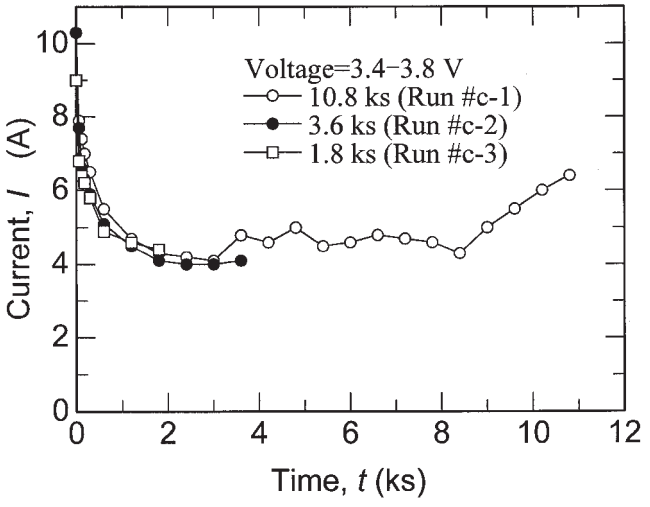

Fig. 6—Change of current during electrolysis under a constant voltage above 3.3 V. Pure $CaCl_2$ was used as listed in Table II.

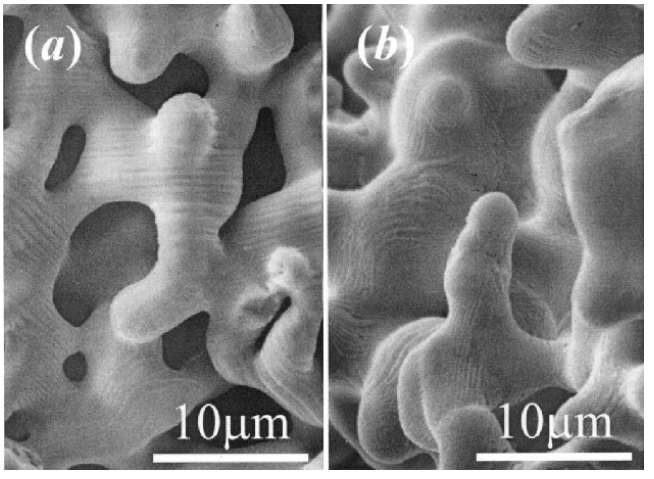

Fig. 7—SEM images of α-Ti: (*a*) run c-1 and (*b*) run c-2.

at the same temperature,[7] the reduction rate of TiO_2 in this experimental cell, *i.e.,* the effective forming rate of Ca, was not so fast as the Ca reduction rate. When we define the current efficiency as the ratio of (the necessary charge to attain the analyzed oxygen level)/(the applied charge during electrolysis), it is evaluated to be 8.8 and 25.5 pct for the samples for 10.6 and for 3.6 ks, respectively (Table II). Parts of the applied charge were consumed for the ohmic heat in the electric leads and bath and for the formation of inefficient Ca. The excess Ca was recombined with Cl_2 gas,

$$\text{In the bath: } \underline{\text{Ca}} + \text{Cl}_2\,(\text{gas}) = \text{CaCl}_2 \qquad [12]$$

or reacted with carbon oxides. The details of the parasitic reactions and current efficiency are discussed in Section IV–D.

B. Electrolysis and Reduction Below 3.0 V

During electrolysis below 3.0 V (lower than the decomposition voltage of $CaCl_2$) and above 2.0 V, only CO_2 gas evolution was observed, as listed in Table II. Figure 8 shows the current change during electrolysis at 1173 K. The current generally dropped at the beginning of electrolysis, then increased gradually. The higher the concentration of CaO that was used, the larger the current was, under the same experimental geometry and the same applied voltage (refer to the "total charge" in Table II). A larger amount of Ca was expected to reduce TiO_2 more effectively. However, α-Ti single phases could be obtained after 10.8 ks, only with the salts with a lower concentration of CaO. When 15 mol pct CaO was used, lower oxides such as $TiO_{0.325}$ or Ti_6O were mixed with α-Ti even after 10.8 ks.

Figure 9 shows the morphology of α-Ti single phases. Grain sizes were similar to the case of $CaCl_2$ electrolysis (Figure 7). A twin structure was never observed in sample f-1, which achieved the minimum oxygen concentration, 2000 ppm O. In the case of short-term electrolysis, lower Ti oxides existed independently from α-Ti particles. A part of the obtained powder was α-Ti single phase (Figure 10(a)), but another part in the same specimen was $TiO_{0.325}$ single phase (Figure 10(b)). The former was characterized by its coarser

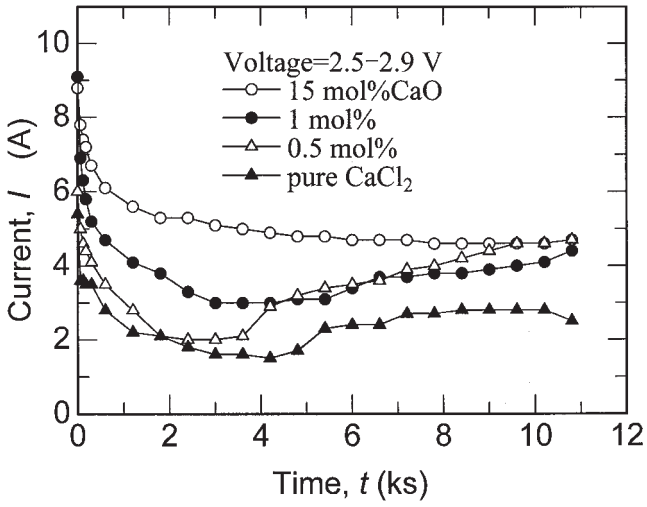

Fig. 8—Change of current during electrolysis under a constant voltage below 3.0 V.

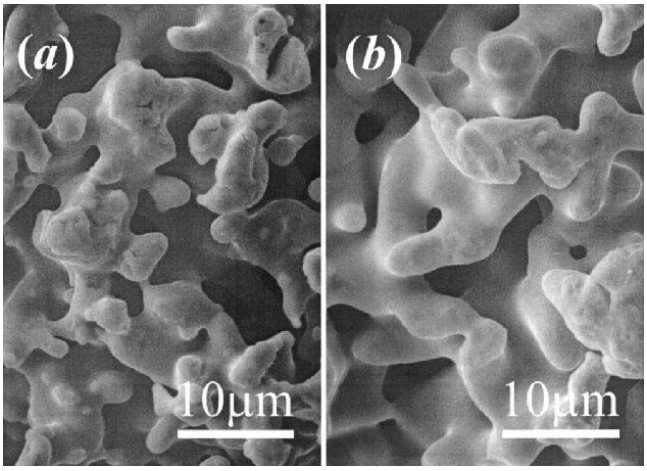

Fig. 9—SEM images of α-Ti: (*a*) run e-1 and (*b*) run f-1.

grains than the latter and by the sintered form. When the powder was identified as $TiO_{0.325}$ or Ti_6O, all the particles were well isolated and smaller in size. The inhomogeneous reduction in the same sample reflects the inhomogeneous distribution of Ca and CaO contents inside the basket-type cathode.

Axler and DePoorter[38] reported that Ca solubility in $CaCl_2$ decreased with the addition of CaO, and that the Ca supply into the $CaCl_2$-CaO melt became slow at >5 mol pct CaO. The slow dissolution of Ca and CaO leads to a higher oxygen concentration in Ti and the local inhomogeneity of oxygen, when the CaO content in the salt is higher.

In the case of pure $CaCl_2$, TiO_2 was reduced to the lower oxide, $TiO_{0.325}$, but α-Ti was not obtained after 10.8 ks of electrolysis. This is because the charge was limited in the electrolysis under a constant voltage. Once a small amount of CaO by the reduction of TiO_2 was served in the $CaCl_2$ melt, Ca would be produced by Eqs. [4] through [7], and it could reduce TiO_2 subsequently. However, the total supplied charge was much smaller than that in the system containing CaO initially.

A quick reduction by Ca produces a region of high CaO concentration, while it hinders the successive dissolution of CaO from the reduced Ti particles and results in the inhomogeneous

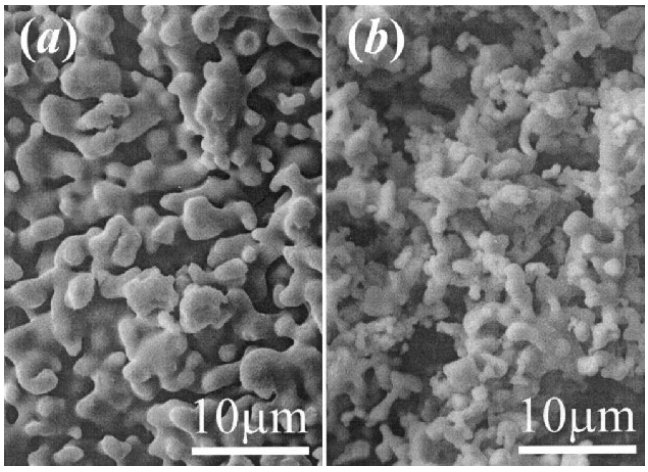

Fig. 10—SEM images of sample e-2, which was obtained in 1 mol pct CaO-$CaCl_2$ by appling 2.7 V for 3.6 ks at 1173 K: (*a*) α-Ti and (*b*) $TiO_{0.325}$.

deoxidation. A lesser amount of CaO does not form enough Ca for reduction. Therefore, it is essential for this process in a single bath to keep a good rate balance among three steps; the thermochemical reduction of TiO_2, the dissolution of CaO, and the electrochemical decomposition of CaO.

C. *Electrolysis using Stainless Steel*

Table III shows the results when a stainless steel basket-type cathode was used as an alternative to the Ti net. The current behaviors were similar to those shown in Figure 8. The obtained black powders were commonly identified as a mixture of α-Ti, TiC, and a small amount of α-Fe. TiO, TiN, or TiC were identified by XRD, because they have the same crystal structure and similar lattice parameters. Because EDX analysis could not find any trace of oxygen or nitrogen, TiC formation was accepted. The origin of carbon is discussed in Section IV–D.

The EDX analysis showed that some α-Ti particles were heavily contaminated by Fe and Ni. This is due to physical contact between the formed Ti and the surrounding stainless steel net. It was confirmed by the fact that some pieces of pure Ti wire were also contaminated when they were immersed in the stainless steel basket for 10.8 ks. Particles of α-Fe were sometimes found. They might come from the corrosion product formed before immersing the steel net, by the fume of $CaCl_2$, or from residual amounts of HCl.

D. *Carbon Precipitation*

The problem encountered mainly in CaO electrolysis was carbon precipitation. Carbon dust was observed in the upper part of the bath and froze as a crust layer about 5 mm thick, in the worst case. The black layer consisted mainly of amorphous carbon and the salt components. $Ca(OH)_2$ and $CaCO_3$ were often found by XRD. They might be formed with the reaction with CaO, moisture, and CO_2 gas in air before the XRD measurement. CaC_2 was never found by XRD. The amount of carbon precipitates during CaO electrolysis was much more than that of $CaCl_2$ electrolysis and was related to neither electrolysis time nor total charge. The cell arrangement, such as the distance between electrodes, affected more strongly the carbon precipitation. The gradual increase of current in Figures 6 and 8 may reflect this reaction related with carbon.

Table III. Experimental Conditions and Results at 1173 K Using the Basket-Type Cathode Consisting of Stainless Steel SUS304

Run	Molten Salt (mol pct)	Voltage (V)	Detected Gas	Time (ks)	Phases Identified by XRD
a-1	$CaCl_2$	3.5 to 3.8	CO_2, Cl_2	10.8	α-Ti, TiC, α-Fe
b-1	15 pct CaO	2.6 to 2.7	CO_2	10.8	α-Ti, TiC, α-Fe
b-2	15 pct CaO	2.3 to 2.4	CO_2	10.8	α-Ti, TiC, α-Fe
b-3	15 pct CaO	2.7 to 2.8	CO_2	10.8	α-Ti, TiC

The carbon precipitates penetrated into the basket-type cathode and contaminated the Ti powder. The surface of the Ti basket reacted partially with carbon, not with the stainless steel basket. This TiC formation from the Ti basket protected the Ti powder inside the cathode from carbon contamination.

Carbon can be formed by the mechanism shown in Eqs. [8] and [9], mentioned in Section II–C. Another mechanism is the following:

$$\text{Near the anode: } \underline{O}^{2-} + CO_2\,(\text{gas}) = CO_3^{2-} \qquad [13]$$

$$\text{In the bath: } 3\,\underline{Ca} + CO_3^{2-} = C + 3Ca^{2+} + 3O^{2-} + 2e^- \qquad [14]$$

The amount of carbon precipitation by Eq. [14] may be more significant at a high CaO concentration or at a high forming rate of $\underline{CaO}$ in reduction, because the solubility of CO_2 gas becomes higher.[54] Because the dependency of C precipitation on CaO content was not clear in this study, the latter mechanism was still uncertain. However, the occurrence of these parasitic reactions consumes a large amount of $\underline{Ca}$, and it significantly decreases the current efficiency.

Ferro *et al.* proposed the use of a porous MgO diaphragm in order to separate CO/CO_2 gas from $\underline{Ca}$.[39,40,41] By analyzing the cell behavior and gas bubbling, we believe that the cell design is a key to solving the matter. In Figure 3, the cathode itself plays a kind of wall to separate the anodic region and cathodic region. The flow of the gas bubbles along the anode should be controlled more precisely to avoid the parasitic reactions.[4,5,6] Another solution is the control of CaO concentration, as given in section IV–E.

E. *Comparison between Electrolysis above and below 3.2 V*

$CaCl_2$ electrolysis requires about a two-times-higher voltage (E) than CaO electrolysis, and the total charge for Cl_2 evolution was larger than that for CO/CO_2 evolution, as listed in Table II. The reduction was completed within 3.6 ks in $CaCl_2$ electrolysis. However, the oxygen concentration in Ti and the current efficiency were better in the case of CaO electrolysis. In our experimental conditions, the amount of O^{2-} coming from TiO_2 was not so large: the increment of CaO concentration was evaluated to be only 1.0 to 1.5 mol pct CaO, even if we assume that the formed CaO was not electrolyzed. This small increase, therefore, does not change the deoxidation rate from α-Ti.

The low current efficiency shows that a large amount of $\underline{Ca}$ was consumed for the back-reaction [12] (>3.2 V) and for reactions [8], [9], and [14] (<3.2 V). The higher quantity of CaO can produce the larger amount of $\underline{Ca}$; however, the excess of $\underline{Ca}$ is consumed by these back- and parasitic reactions. At a lower concentration of CaO, a lesser amount of $\underline{Ca}$ is formed per unit time. It reacts more effectively with TiO_2 powder located near the cathode. A low CaO concentration is suitable for deoxidation, as shown in Eq. [10], and decreases the possible formation of CO_3^{2-}.

F. *Comparison with Previous Works*

Some other trials were reported to produce Ti electrochemically from TiO_2 in $CaCl_2$. Because TiO_2 is insoluble in the molten salt, the dissolution of TiO or $CaTiO_3$ into $CaCl_2$ was used.[55,56] Oki and Inoue connected a cathode wire directly to TiO_2 in $CaCl_2$ and reported the formation of Ti.[57] Recently, Chen *et al.* explained it as a simple mechanism of a direct electrolysis of cathodic TiO_2.[58,59,60]

$$\text{At the cathode: } TiO_2 + 2e = Ti + \underline{O^{2-}} \qquad [15]$$

$$\text{At the anode: } 2\underline{O^{2-}} = O_2\,(\text{gas}) + 2e \qquad [16]$$

where the role of anions was not considered. The comparison between this FFC (Fray-Farthing-Chen) process and our proposal is illustrated in Figure 11. Although its operating mechanisms are different, the bath, carbon anode, and applied voltage are apparently similar. The FFC process uses the sintered pellets of TiO_2 as the cathode, and the oxygen diffusion in cathodic Ti plate is required.

We believe that Ca ions play a certain role in reactions, first, because $CaTiO_3$ was sometimes formed. Second, at the applied voltage in the FFC process, Ca from $\underline{CaO}$ can precipitate on the surface of the TiO_{2-x} cathode. If the evolved oxygen gas in Eq. [13] reacts with the anodic carbon to form CO/CO_2 gas, the total reactions in the FFC process and our proposal become the same reaction, shown in Eq. [11].

Our process does not need a direct electrical contact between TiO_2 and the cathodic lead, and TiO_2 can be fed in powder form, which is suitable for oxygen removal because there is no requirement of oxygen diffusion in a long distance. A short-term reduction and deoxidation can be possible using our principle.

G. *Verification of Calciothermic Reduction*

A preliminary experiment showed that $\underline{Ca}$ worked in our cell: TiO_2 was filled in a small Y_2O_3 crucible and placed inside the Ti basket-type cathode. Because Y_2O_3 is an electronic insulator and thermodynamically more stable than CaO, the TiO_2 powder was electronically isolated from the cathodic lead. After holding for 10.8 ks at 1173 K, the powder at the upper part of the Y_2O_3 crucible changed to α-Ti, TiO, Ti_2O_3, and $CaTiO_3$, although TiO_2 at the bottom of the crucible remained unchanged. This fact could not be explained by the FFC mechanism. Simultaneously, the inhomogeneity in this Y_2O_3 crucible proved that a uniform

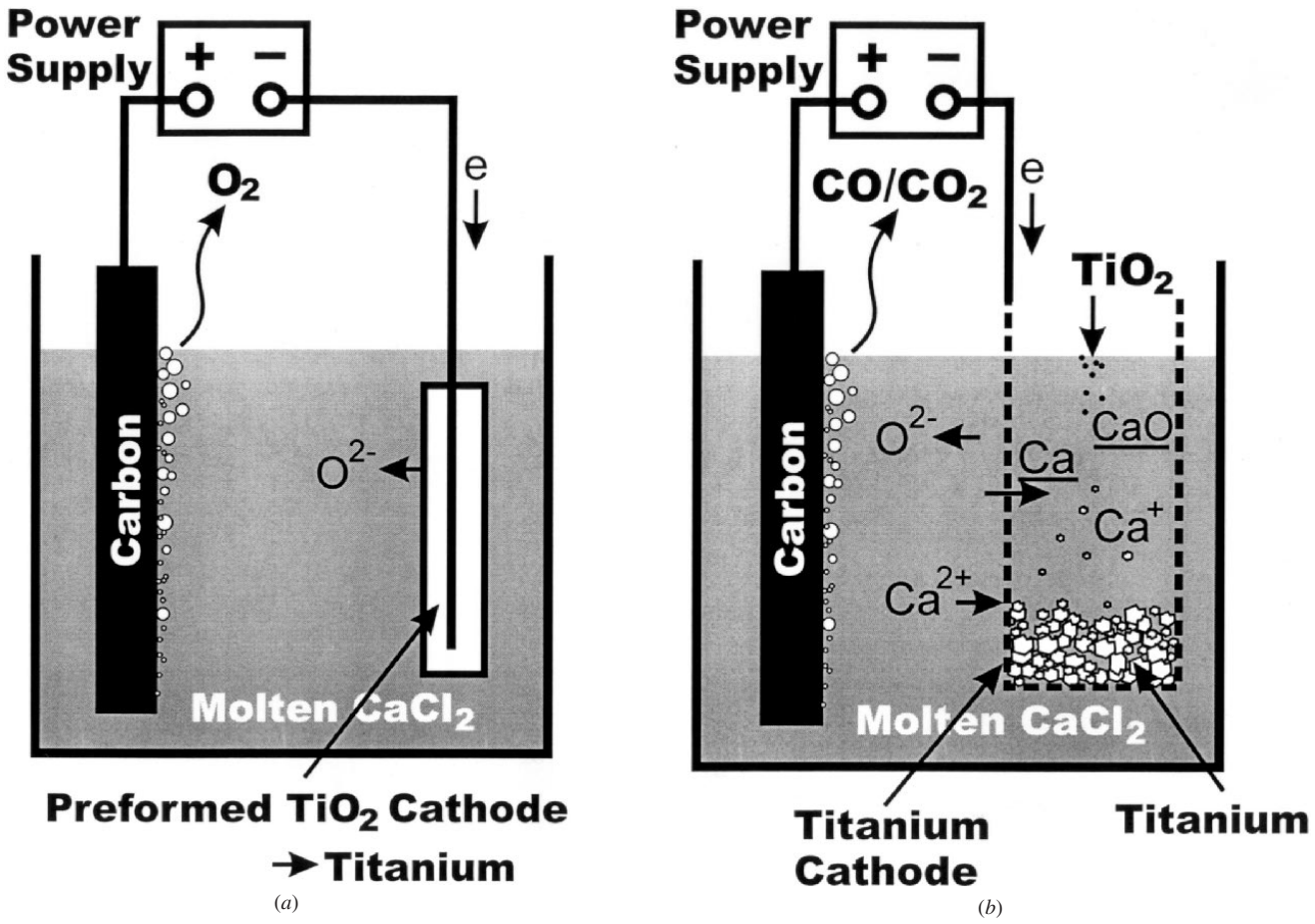

Fig. 11—Comparison of the mechanism in (*a*) FFC process[58,59,60] and (*b*) our proposal.

dispersion of TiO_2 powder in $CaCl_2$ or the exposure of TiO_2 to $CaCl_2$ is a technical key to obtain good homogeneity.

V. CONCLUSIONS

A concept was proposed that Ti granular sponge could be produced directly from TiO_2 powder, by combining both the calciothermic reduction and the *in-situ* electrolysis of CaO in the CaO-$CaCl_2$ bath, as shown in Figure 3. Theoretical and technical requirements for this concept were described in detail, and the potential to obtain a Ti powder suitable for an industrial oxygen level was analyzed, based on the previous studies.

Experimentally, the concept was tested using the basket-type cathode, in which TiO_2 was filled. The reduction of TiO_2 per unit time was superior in the electrolysis of Cl_2 gas evolution ($E > 3.2$ V at 1173 K), while the residual oxygen level in Ti was better in the electrolysis of CO/CO_2 gas evolution ($E < 3.2$ V). A level of 2000 ppm oxygen in α-Ti was achieved within 10.8 ks using the 0.5 to 1 mol pct CaO-$CaCl_2$ melt.

Parasitic reactions such as carbon precipitation and the back-reaction lowered the current efficiency to 8 to 25 pct. These reactions will be minimized by the modification of cell design and by a good rate balance among three steps: the calciothermic reduction of TiO_2, the dissolution of CaO, and the electrochemical decomposition of CaO.

ACKNOWLEDGMENTS

The authors thank Mr. T. Unesaki for SEM-EDX analysis, Mr. S. Fukui for experimental assistance, and Mr. P.Y. Gear for statements on the manuscript. This work was financially supported in part by the Japan Titanium Society, Sumitomo Titanium Co. Ltd., Toho Titanium Co. Ltd., Nippon Light Metals Ltd., and Grants-in-Aid for Scientific Research under Contract No. 14205109.

REFERENCES

1. W. Kroll: *Trans. Electrochem. Soc.,* 1940, vol. 78, pp. 35–47.
2. K. Ono: *Titanium Jpn.,* 2000, vol. 48 (1), pp. 13–15.
3. K. Ono and R.O. Suzuki: *Proc. Symp. on Emerging Technologies for Metals Extraction, EPD Congr. 2001,* 2001 TMS Annual Meeting, New Orleans, LA, P.R. Taylor, ed., TMS, Warrendale, PA, 2001, pp. 79–88.
4. K. Ono and R.O. Suzuki: *Mater. Jpn.,* 2002, vol. 41 (1), pp. 28–31.
5. K. Ono and R.O. Suzuki: *JOM Mem. J. Min. Met. Mater. Soc.,* 2002, vol. 54 (2), pp. 59–61.
6. K. Ono and R.O. Suzuki: *Titanium Jpn.,* 2002, vol. 50 (2), pp. 105–08.
7. R.O. Suzuki and S. Inoue: *Metall. Mater. Trans. B,* 2003, vol. 34B, pp. 277–85.
8. R.O. Suzuki and K. Ono: *Proc. 13th Int. Symp. on Molten Salt,* H.C. Delong, R.W. Bradshaw, M. Matsunaga, G.R. Stafford, and P.C. Trulove, eds., The Electrochemical Society, Penningston, NJ, 2002, pp. 810–21.
9. A. Roine: *HSC Chemistry for Windows,* ver. 4.1, Outokump Research Oy, Pori, Finland, 2000.
10. H. Okamoto: *Desk Handbook Phase Diagrams for Binary Alloys,* ASM INTERNATIONAL, Materials Park, OH, 2000.

11. O. Kubaschewski and W.A. Dench: *J. Inst. Met.,* 1953, vol. 82, pp. 87–91.
12. K. Ono, T.H. Okabe, M. Ogawa, and R.O. Suzuki: *Tetsu-to-Hagané,* 1990, vol. 76 (4), pp. 568–75.
13. W. Kroll: *Z. Anorg. Allgem. Chem.,* 1937, vol. 234, pp. 42–50.
14. S. Miyazaki, T. Oishi, and K. Ono: *Proc. 5th. World Conf. on Titanium,* Munich, Germany, Sept. 10–14, 1984, G. Lütjering, U. Zwicker, and W. Bunk, eds., Deutsche Geselschaft für Metallk., Oberursel, Germany, 1985, pp. 2657–63.
15. K. Ono and S. Miyazaki: *J. Jpn. Inst. Met.,* 1985, vol. 49 (10), pp. 871–75.
16. R.O. Suzuki, M. Ogawa, T. Oishi, and K. Ono: *Proc. 6th World Conf. on Titanium 1988,* Cannes, France, 1988, Soc. Franc. Metall., Paris, 1989, vol. II, pp. 701–06.
17. T.H. Okabe, R.O. Suzuki, T. Oishi, and K. Ono: *Mater: Trans. JIM,* 1991, vol. 32 (5), pp. 485–88.
18. H. Niiyama, Y. Tajima, F. Tsukihashi, and N. Sano: *J. Less-Common Met.,* 1991, vol. 169, pp. 209–16.
19. I. Obinata, Y. Takeuchi, and S. Saikawa: *Trans. ASM,* 1960, vol. 52, pp. 1072–83.
20. P.P. Alexander: U.S. Patent 2.038.402, 1936; U.S. Patent 2.043.363, 1936; and U.S. Patent 2.082.134, 1937.
21. B. Neumann, C. Kröger, and H. Jüttner: *Z. Elektrochem.,* 1935, vol. 41 (10), pp. 725–36.
22. W.D. Threadgill: *J. Electrochem. Soc.,* 1965, vol. 112 (6), pp. 632–33.
23. D.A. Wenz, I. Johnson, and R.D. Wolson: *J. Chem. Eng. Data,* 1969, vol. 14 (2), pp. 250–52.
24. G.S. Perry and L.G. MacDonald: *J. Nucl. Mater.,* 1985, vol. 130, pp. 234–41.
25. T. Ohshima, R.O. Suzuki, T. Yagura, and K. Ono: *Proc. 2000 Powder Metallurgy World Congr.,* Kyoto, Japan, Nov. 13–18, 2000, K. Kosuge and H. Nagai, eds., Japan Society Powder and Powder Metallurgy, Tokyo, 2001, pp. 532–35.
26. W.Z. Wade and T. Wolf: *J. Nucl. Sci. Technol.,* 1969, vol. 6, pp. 402–07.
27. R.A. Sharma: *J. Met.,* 1987, vol. 2, pp. 33–37.
28. R.A. Sharma and R.N. Seefruth: *J. Electrochem. Soc.,* 1988, vol. 135 (1), pp. 66–71.
29. R.A. Sharma and R.N. Seefruth: *Metall. Trans. B,* 1989, vol. 20B (6), pp. 805–13.
30. *Metals Databook,* Japan Institute of Metals ed., 2nd ed., Maruzen, Tokyo, 1984, pp. 9, 15, 34, and 68.
31. Y.S. Touloukian, R.K. Kirby, R.E. Taylor, and T.Y.R. Lee: *Thermal Expansion, Nonmetallic Solid,* IFI/Plenum, New York, NY, 1977, pp. 49 and 392–97.
32. D.T. Peterson and J.A. Hinkebein: *J. Phys. Chem.,* 1959, vol. 63, pp. 1360–63.
33. R.A. Sharma: *J. Phys. Chem.,* 1970, vol. 74 (22), pp. 3896–900.
34. V. Dosaj, C. Aksaranan, and D.R. Morris: *J. Chem. Soc. Faraday Trans.,* 1975, vol. 71, pp. 1083–98.
35. H. Fischbach: *Steel Res.,* 1985, vol. 56 (7), pp. 365–68.
36. L.-I. Staffansson and D. Sichen: *Scand. J. Metall.,* 1992, vol. 21, pp. 165–71.
37. A.I. Zaitsev and B.M. Mogutnov: *Metall. Mater. Trans., B,* 2001, vol. 32B, pp. 305–11.
38. K.M. Axler and G.L. DePoorter: *Mater. Sci. Forum,* 1991, vol. 73–75, pp. 19–24.
39. P.D. Ferro, B. Mishra, D.L. Olson, and W.A. Averill: *Waste Management,* 1997, vol. 17, pp. 451–61.
40. P.D. Ferro, B. Mishra, D.L. Olson, and W.A. Averill: *Trans. Ind. Inst. Met.,* 1998, vol. 51, pp. 69–77.
41. P.D. Ferro, B. Mishra, and W.A. Averill: in *Light Metals 1991,* E.L. Rooy, ed., TMS, Warrendale, PA, 1990, pp. 1197–1203.
42. G.J. Kipouros and R.A. Sharma: *J. Electrochem. Soc.,* 1990, vol. 137, pp. 3333–38.
43. M. Kunitomi: *J. Chem. Soc. Jpn., Pure Chem. Sec.,* 1950, vol. 71, pp. 40–43.
44. R. Lorenz: *Trans. Am. Electrochem. Soc.,* 1904, vol. 6, pp. 160–61.
45. H.-H. Emons and D. Richter: *Z. Anorg. Allg. Chem.,* 1965, vol. 339, pp. 91–98.
46. A.S. Dworkin, H.R. Bronstein, and M.A. Bredig: *J. Phys. Chem.,* 1966, vol. 70 (7), pp. 2384–88.
47. T.H. Okabe, R.O. Suzuki, T. Oishi, and K. Ono: *Tetsu-to-Hagané,* 1991, vol. 77 (1), pp. 93–99.
48. T.H. Okabe, T. Oishi, and K. Ono: *J. Alloys Compounds,* 1992, vol. 184, pp. 43–56.
49. T.H. Okabe, M. Nakamura, T. Ueki, T. Oishi, and K. Ono: *Bull. Jpn. Inst. Met.,* 1992, vol. 31 (4), pp. 315–17.
50. T.H. Okabe, T.N. Deura, T. Oishi, K. Ono, and D.R. Sadoway: *J. Alloys Compounds,* 1996, vol. 237, pp. 150–54.
51. R.O. Suzuki, M. Aizawa, and K. Ono: *J. Alloys Compounds,* 1999, vol. 288, pp. 173–82.
52. T.H. Okabe, M. Nakamura, T. Oishi, and K. Ono: *Metall. Trans. B,* 1993, vol. 24B, pp. 449–56.
53. K. Hirota, T.H. Okabe, F. Saito, Y. Waseda, and K.T. Jacob: *J. Alloys Compounds,* 1999, vol. 282, pp. 101–08.
54. M. Maeda and A. McLean: *ISS Trans.,* 1987, vol. 8, pp. 23–27.
55. M.E. Sibert, Q.H. McKenna, M.A. Steinberg, and E. Wainer: *J. Electrochem. Soc.,* 1955, vol. 102 (5), pp. 252–62.
56. S. Takeuchi and O. Watanabe: *J. Jpn. Inst. Met.,* 1964, vol. 28 (9), pp. 549–54.
57. T. Oki and H. Inoue: *Mem. Fac. Eng., Nagoya Univ.,* 1967, vol. 19 (1), pp. 164–66.
58. G.Z. Chen, D.J. Fray, and T.W. Farthing: *Nature,* 2000, vol. 407, pp. 361–64.
59. G.Z. Chen, D.J. Fray, and T.W. Farthing: *Metall. Mater. Trans. B,* 2001, vol. 32B (6), pp. 1041–52.
60. D.J. Fray: *JOM Mem. J. Min. Met. Mater. Soc.,* 2001, vol. 53 (10), pp. 26–31.